J. Phys. B: At. Mol. Opt. Phys. **23** (1990) 3909-3924. Printed in the UK

Total and differential charge transfer cross sections in $H^+ + Na(3s)$ or $Na^*(3p)$ collisions

C Courbin†, R J Allan‡, P Salas§ and P Wahnon§

† Laboratoire de Dynamique Moléculaire et Atomique‖, Université Pierre et Marie Curie, 4 Place Jussieu, T12 E5, 75252 Paris, France

‡ Advanced Research Computing Group, SERC, Daresbury Laboratory, Warrington WA4 4AD, UK

§ Departamento TEAT, ETSI Telecomunicacion, Universidad Politecnica, 28040 Madrid, Spain

Received 17 April 1990, in final form 18 July 1990

Abstract. Proton-sodium charge transfer is studied, using 9- and 19-state adiabatic molecular bases and the impact parameter method, in the energy range 0.5-5 keV. The dynamical radial and rotational coupling terms and a common translation factor (CTF) are included. The effect of the choice of the coordinate centre on the total charge exchange cross sections to $H(n=2)$ is clearly demonstrated when no CTF is included. The alignment dependence of the capture to $H(n=2)$ is obtained and is satisfactorily compared with the atomic expansion calculations. State-to-state charge exchange differential cross sections are calculated; the alignment and orientation effects are expected to be observable at the collision energy 0.5 keV where they are spread out at scattering angles $\theta > 0.1°$.

1. Introduction

The electron capture process from the ground state of Na atoms:

$$H^+ + Na(3s) \rightarrow H(n=2) + Na^+ \qquad \Delta E = -1.74\ \text{eV} \qquad \text{(R1)}$$

has been studied extensively theoretically and experimentally due to a long-standing disagreement between the theoretical and the experimental total charge exchange cross sections. The conclusion of the most recent studies from molecular orbital (MO) calculations (Allan 1986 and references therein) and atomic orbitals (AO) calculations (Fritsch 1984, Shingal *et al* 1986) cast doubt on the reliability of the MO calculations of Kimura *et al* (1982a, b) and the measurements of Nagata (1983). The calculations of Kubach and Sidis (1981) seem for different reasons to be less satisfactory than the more recent results, which are consistent with each other and agree with the experiments of Gruebler *et al* (1970), McCullough (1978), Anderson *et al* (1979) and Ebel and Salzborn (1983) for the energy range $0.2 < E < 6$ keV. Results for reaction (R1) with a MO basis have been discussed by Allan (1986) (hereafter referred to as I).

‖ CNRS associate laboratory (URA 774).

0953-4075/90/213909+16$03.50

Using the same model as in I we study the reaction:

$$H^+ + Na^*(3p, m) \rightarrow H(n=2) + Na^+ \qquad \Delta E = 0.36 \text{ eV} \tag{R2}$$

which is of interest because of the possibility of preparing the initial state by a laser. In a first set of experiments the Ly_α radiation was observed after the collision (Kushawaha *et al* 1980, Kushawaha 1983), their results at $E > 30$ eV are in contradiction with recent calculations of total cross sections for charge transfer from Na(3s) to H*(2p) and Na*(3p) to H*(2p) by Allan *et al* (1986) (hereafter referred to as II). More recent experiments of Aumayr and Winter (1987) and Aumayr *et al* (1987) tend to confirm the data of II, as also do the experiments of Finck *et al* (1988).

Another type of experiment has been performed by Royer *et al* (1988): a time-of-flight technique enables the identification of all the $H(n) + Na^+$ channels populated in the collision and when the Na(3p) target is prepared with a well defined alignment using laser pumping. One aim of the present paper is to get the sublevel $H(n=2)$ total cross sections in the MO model, partially studied in II at one energy, $E = 0.5$ keV. We have calculated the charge exchange cross sections for H(2s), $H(2p_0, 2p_{\pm 1})$ products from an initial state Na(3s) or $Na(3p_0, 3p_{\pm 1})$ with more accurate asymptotic amplitudes by exactly taking account of the Stark and rotational couplings, which can affect the sublevel populations. Using both a 9- and 19-state MO basis, some effects of the essential electron translational factor are noted for reactions (R1) and (R2). The initial alignment dependence of the capture to $H(n=2)$ is satisfactorily compared with the experimental result (Richter *et al* 1990, following paper). The charge exchange probabilities and differential cross sections are presented and the most important transition mechanisms are discussed for this collision system.

2. General formalism

2.1. Collision model

The quasi-classical impact parameter model for nuclear motion is used and the electronic wavefunction is developed on a molecular basis. The basis was described by Allan (1986) in whose work a model potential method was applied to describe the outer electron of the system in the field of the two cores. As the perturbed stationary state method fails to take into account transfer of the momentum of the electron and the reluctance of electronic eigenfunctions to follow the rotation of an internuclear axis at even moderate speeds, a modified basis set has been proposed including electron translation factors where the wavefunction is expanded on the molecular state χ_n:

$$\Psi_n = \chi_n \exp(i g_n(\boldsymbol{r}, \boldsymbol{R})) \tag{1}$$

where $\boldsymbol{r}$ and $\boldsymbol{R}$ are respectively the electronic and the nuclear coordinates. By allowing g_n to depend on both $\boldsymbol{r}$ and $\boldsymbol{R}$ it is possible to choose g_n independent of state n, as first proposed by Schneiderman and Russek (1969), reconsidered and tested by Errea *et al* (1982). We therefore improve the asymptotic behaviour of the stationary wavefunction by the inclusion of a common translation factor (CTF) as described by Allan and Hanssen (1985):

$$U(\boldsymbol{r}, \boldsymbol{R}) = f(\boldsymbol{r}, \boldsymbol{R})\boldsymbol{v} \cdot \boldsymbol{r} - \tfrac{1}{2} f^2(\boldsymbol{r}, \boldsymbol{R}) v^2 t \tag{2}$$

with

$$f(\boldsymbol{r}, \boldsymbol{R}) = Rz/(R^2+\beta^2) \qquad \text{and} \qquad z = \hat{\boldsymbol{R}} \cdot \boldsymbol{r}. \tag{3}$$

The coupled equations can be deduced:

$$\begin{aligned} \mathrm{i}\frac{\mathrm{d}a^m}{\mathrm{d}t} = \Bigg[& \left\langle \chi_m \middle| \varepsilon_m - \mathrm{i}\frac{\mathrm{d}R}{\mathrm{d}t}\frac{\partial}{\partial R} + \mathrm{i}\frac{\mathrm{d}\gamma}{\mathrm{d}t}\mathrm{i}L_y \middle| \chi_n \right\rangle \\ & - \frac{\mathrm{i}}{R}\left\langle \chi_m \middle| z\frac{\partial}{\partial z} \middle| \chi_n \right\rangle \frac{\mathrm{d}R}{\mathrm{d}t} - \mathrm{i}\left\langle \chi_m \middle| x\frac{\partial}{\partial z} + z\frac{\partial}{\partial x} \middle| \chi_n \right\rangle \frac{\mathrm{d}\gamma}{\mathrm{d}t} \\ & + 1.5\langle \chi_m | x^2 | \chi_n \rangle \left(\frac{\mathrm{d}\gamma}{\mathrm{d}t}\right)^2 \Bigg] a^n \qquad \text{for all } m \end{aligned} \tag{4}$$

where a body-fixed reference frame with z initially in the projectile velocity direction is assumed and where

$$R^2 = b^2 + v^2t^2 \tag{5}$$

defines the relation between R, $z = vt$ and the impact parameter b, γ is the angle between the incident velocity $\boldsymbol{v}$ and the internuclear $\boldsymbol{R}$ oriented from the target to the projectile.

We shall consider the modified matrix elements in the following discussion:

$$H_1 = \left\langle \chi_m \middle| \frac{\partial}{\partial R} + \frac{z}{R}\frac{\partial}{\partial z} \middle| \chi_n \right\rangle \tag{6}$$

$$H_2 = \left\langle \chi_m \middle| \mathrm{i}L_y - \left(x\frac{\partial}{\partial z} + z\frac{\partial}{\partial x} \right) \middle| \chi_n \right\rangle. \tag{7}$$

As we consider collisions involving electron capture by an incident proton into $H(n=2)$, we treat exactly the problem of the long-range mixing of degenerate states of the same symmetry due to the proximity of the alkali ion. It has already been pointed out by Sidis and Kubach (1978) that the corresponding phase integral has to be included to get the metastable fraction of H(2s) in Cs-H^+ charge transfer. The linear Stark effect induces a large coupling between H(2s) and H(2p) that is first order in the electric field strength and must be included in the evolution matrix **U** in order to find the correct final state distribution in $H(n=2)$. Added to the A/R^2 ($A = 3$ au for the H atoms) Stark coupling is the rotational coupling term $\mathrm{i}B/R^2$ with $B = vb\langle \mathrm{i}L_y \rangle$ between any $|p\Sigma\rangle$ and $|p\Pi^+\rangle$ quasi-degenerate states (in the collision plane xOz). The coupling matrix in the body-fixed frame is:

$$\mathbf{T} = \frac{1}{R^2}\begin{pmatrix} 0 & A & 0 \\ A & 0 & -\mathrm{i}B \\ 0 & \mathrm{i}B & 0 \end{pmatrix}. \tag{8}$$

This matrix can be diagonalized by the transformation matrix **S**:

$$\mathbf{S} = \frac{1}{[2(A^2+B^2)]^{1/2}}\begin{pmatrix} A & A & \mathrm{i}B\sqrt{2} \\ (A^2+B^2)^{1/2} & -(A^2+B^2)^{1/2} & 0 \\ \mathrm{i}B & \mathrm{i}B & A\sqrt{2} \end{pmatrix}. \tag{9}$$

So the propagator **U** can be deduced:

$$\mathbf{U}(z_0, z) = \begin{pmatrix} \frac{A^2}{C^2}\cos\phi + \frac{B^2}{C^2} & \mathrm{i}\frac{A}{C}\sin\phi & \mathrm{i}\frac{AB}{C^2}\cos\phi + \mathrm{i}\frac{AB}{C^2} \\ \mathrm{i}\frac{A}{C}\sin\phi & \cos\phi & \frac{B}{C}\sin\phi \\ \mathrm{i}\frac{AB}{C^2}\cos\phi - \mathrm{i}\frac{AB}{C^2} & -\frac{B}{C}\sin\phi & \frac{B^2}{C^2}\cos\phi + \frac{A^2}{C^2} \end{pmatrix} \tag{10}$$

where

$$C^2 = A^2 + B^2 \qquad \text{and} \qquad \phi = \frac{1}{v}\int_{z_0}^{z} \frac{(A^2+B^2)^{1/2}}{R^2}\,\mathrm{d}z.$$

The coupled equations (4) are solved up to $z_0 = 40$ au for each impact parameter and the final amplitudes $b^m(\infty)$ are obtained by:

$$a^m(\infty) = \mathbf{U}(z_0, \infty)a^m(z_0). \tag{11}$$

A similar transformation is needed for the initial states in the general case. We can therefore give the distribution of the flux over the final $|n, l, m\rangle$ state, as shown for total cross sections in section 3 and for probability amplitudes in section 4.

2.2. Total charge exchange cross section with CTF from Na(3p) excited by a linearly polarized laser*

As we use a wavefunction developed on a molecular basis the atomic substates of different M_L must be rotated to the molecular substates: $3p\Sigma$, $3p\Pi^+$, $3p\Pi^-$. From solving the impact parameter equations (4) (with 9 or 19 states) we obtain the $\sigma_\Sigma(n=2)$, $\sigma_{\Pi^+}(n=2)$ and $\sigma_{\Pi^-}(n=2)$ cross sections meaning the initial state is $3p\Sigma_{Na}$, $3p\Pi^+_{Na}$, $3p\Pi^-_{Na}$ respectively) by summing up the possible final substates of $H(n=2)$: $2s\Sigma$, $2p\Sigma$, $2p\Pi^+$, $2p\Pi^-$ allowed by symmetry selection rules:

$$\begin{aligned} \sigma_\Sigma(n=2) &= \sigma_\Sigma(2s\Sigma) + \sigma_\Sigma(2p\Sigma) + \sigma_\Sigma(2p\Pi^+) \\ \sigma_{\Pi^+}(n=2) &= \sigma_{\Pi^+}(2s\Sigma) + \sigma_{\Pi^+}(2p\Sigma) + \sigma_{\Pi^+}(2p\Pi^+) \\ \sigma_{\Pi^-}(n=2) &= \sigma_{\Pi^-}(2p\Pi^-). \end{aligned} \tag{12}$$

The linearly perpendicular polarized light excites the atom in a statistical mixture of $|3p\Pi^+\rangle$ and $|3p\Pi^-\rangle$: 0.5, 0.5 and the total charge exchange cross section which corresponds to an average over all the directions of the collision plane is:

$$\sigma_\Pi(n=2) = \tfrac{1}{2}[\sigma_{\Pi^+}(n=2) + \sigma_{\Pi^-}(n=2)]. \tag{13}$$

The $\sigma_\Sigma(n=2)$ and $\sigma_\Pi(n=2)$ cross sections are obtained from (12) and (13) and lead to the alignment of the Na*(3p) state for the capture to $H(n=2)$.

3. Total charge exchange cross sections

3.1. Molecular expansion without CTF

Many calculations have been performed without CTF in some theoretical models for this system but they have not yet been compared with a calculation made with the same expansion and including a CTF to test the effect of the added matrix elements.

If no CTF is included the dynamical couplings depend on the chosen electron coordinate origin C and generally have spurious long-range behaviour. We temporarily circumvent the problem as in some other works (Taulbjerg and Briggs 1975, Wahnon *et al* 1986) by choosing the coordinate centre $C = \nu$ when $\nu = \nu'$ and $C = \nu$ or $C = \nu'$ when $\nu \neq \nu'$, ν indicating one of the nucleus centres, so that we can test the role of the choice of the coordinate centre and at the same time the limit of the use of the molecular expansion without CTF.

3.1.1. Electron capture from Na(3s). The two different choices for the coordinate centre C are the H nucleus and the centre of mass of the system. First a comparison of the dynamical matrix elements for these two different coordinate centres shows (figure 1(*a*)) that the $\langle 3s\Sigma|\, d/dR|2s\Sigma, 2p\Sigma\rangle$ and the $\langle 3s\Sigma|iL_y|2p\Pi^+\rangle$ matrix elements are much smaller when C = centre of mass (CM) than C = H nucleus, especially in the interacting region $8 < R < 20$ au. We can expect that the total charge exchange cross section for production of $H(n = 2)$ will be much larger when C = H than when C = CM.

The charge exchange cross section to $H(n = 2)$ calculated with the inclusion of the CTF (I) is compared with the present result in figure 3(*a*). The three types of calculation converged to the same value for $E < 0.5$ keV ($v = 0.2$ au). So, below 0.5 keV the molecular expansion is valid for studying the reaction (R1) without inclusion of the

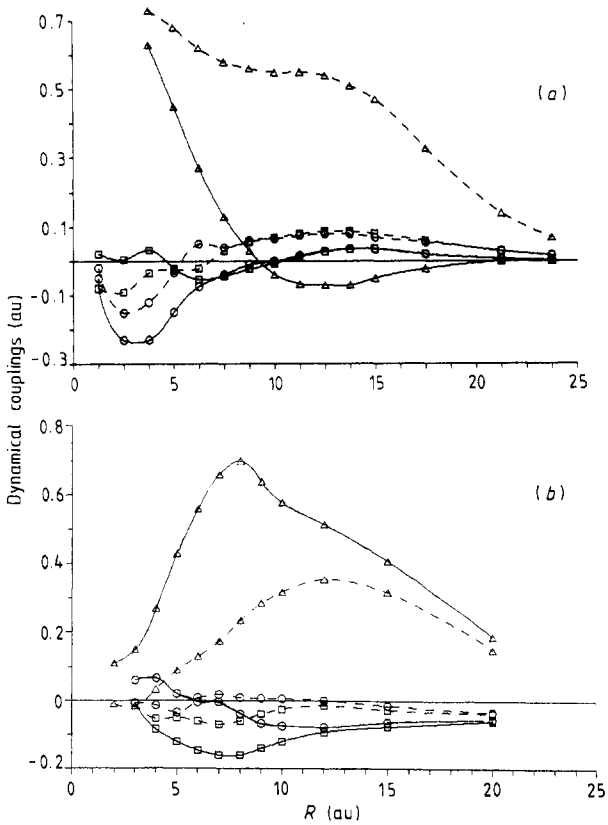

Figure 1. Radial and rotational matrix elements without CTF: ——, coordinate centre C = CM; – – –, C = H. (*a*) △, $\langle 3s\Sigma|iL_y|2p\Pi\rangle$; ○, $\langle 3s\Sigma|\,\partial/\partial R|2s\Sigma\rangle$; □, $\langle 3s\Sigma|\,\partial/\partial R|2p\Sigma\rangle$. (*b*) △, $\langle 3p\Sigma|iL_y|2p\Pi\rangle$; ○, $\langle 3p\Sigma|\,\partial/\partial R|2s\Sigma\rangle$; □, $\langle 3p\Sigma|\,\partial/\partial R|2p\Sigma\rangle$.

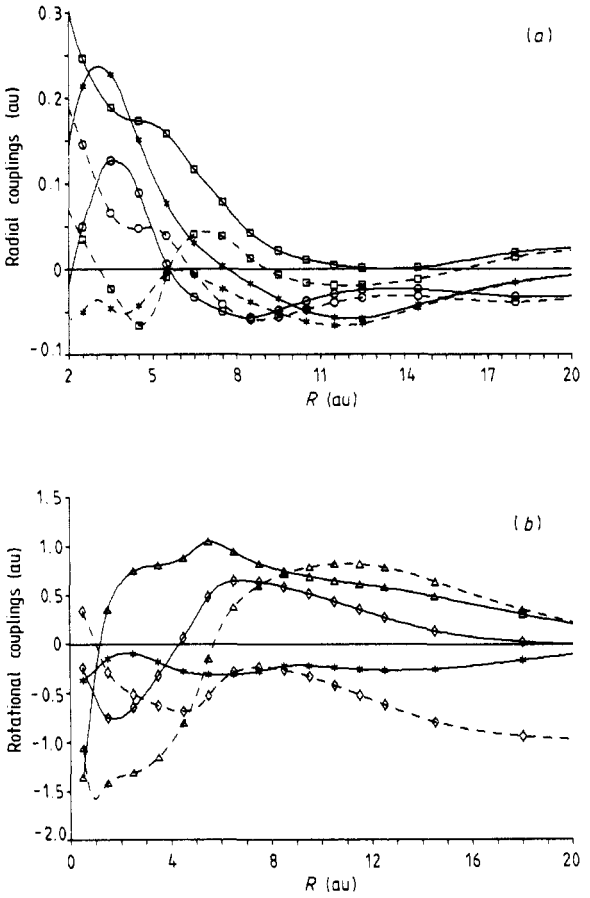

Figure 2. (a) Modified radial matrix elements H_1 (equation (6)): —*—, $\langle 2s_H|H_1|3s\Sigma_{Na}\rangle$; --*--, $\langle 2p\Sigma_H|H_1|3s\Sigma_{Na}\rangle$; —○—, $\langle 3p\Sigma_{Na}|H_1|2s\Sigma_H\rangle$; --○--, $\langle 3p\Sigma_{Na}|H_1|2p\Sigma_H\rangle$; —□—, $\langle 4s\Sigma_{Na}|H_1|2s\Sigma_H\rangle$; --□--, $\langle 4s\Sigma_{Na}|H_1|2p\Sigma_H\rangle$. ($b$) Modified rotational matrix elements H_2 (equation (7)): —◇—, $\langle 2p\Pi_H|H_2|2s\Sigma_H\rangle$; --◇--, $\langle 2p\Pi_H|H_2|2p\Sigma_H\rangle$; —△—, $\langle 3p\Pi_{Na}|H_2|2s\Sigma_H\rangle$; --△--, $\langle 3p\Pi_{Na}|H_2|2p\Sigma_H\rangle$; —*—, $\langle 3p\Sigma_{Na}|H_2|2p\Pi_H\rangle$.

correction of the CTF for the asymptotic behaviour. It is noticeable that the CTF result is just at a mean value between the calculation with $C = H$ and $C = CM$: as if *the equivalent coordinate centre for matrix elements was the geometric centre of the molecule.*

3.1.2. Electron capture from Na(3p).* If the initial state is Na*(3p) then the matrix elements (figure 1(b)) for the two different choices of coordinate centre are in an inverse relative position (compared with the matrix elements involving the $|3s_{Na}\rangle$ state):

$$\left\langle 3p\Sigma\left|\frac{d}{dR}\right|2s\Sigma\right\rangle_{CM} \gg \left\langle 3p\Sigma\left|\frac{d}{dR}\right|2s\Sigma\right\rangle_{H}$$

and

$$\langle 3p\Sigma|iL_y|2p\Pi\rangle_{CM} \gg \langle 3p\Sigma|iL_y|2p\Pi\rangle_{H}$$

when $6 < R < 12$ au.

The cross sections $\sigma_\Sigma(n=2)$ and $\sigma_\Pi(n=2)$ defined by (12) and (13) are reported in figure 4(a). The cross sections with initial state $|3p\Pi\rangle$ are four times larger when

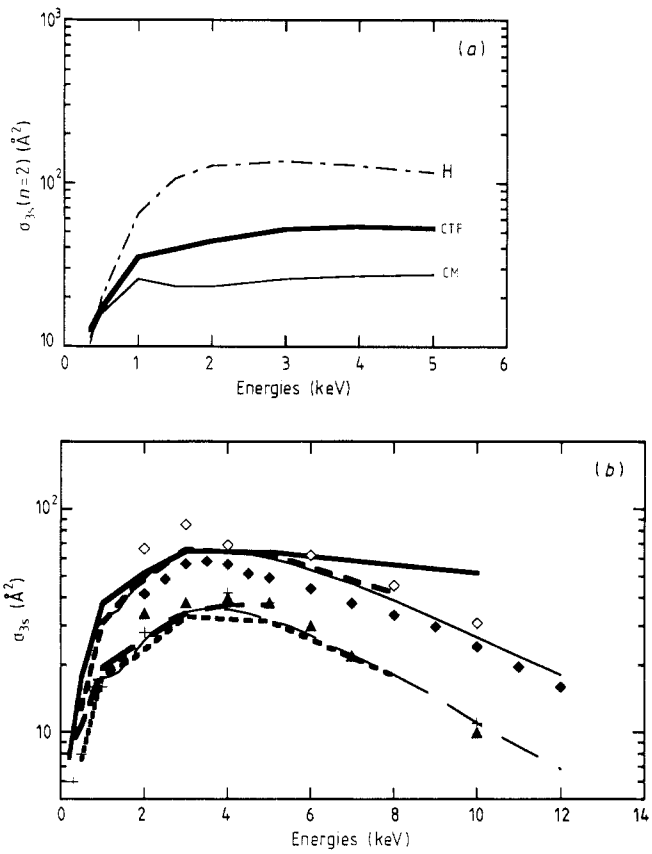

Figure 3. (*a*) Charge exchange cross section $\sigma_{3s}(n=2)$: ——, without CTF and $C=$CM; ——, with CTF; — — —, without CTF and $C=$H. (*b*) Charge exchange cross section $\sigma_{3s}(n=2)$: ——, AO calculations (Shingal *et al* 1986); – – –, AO calculations (Fritsch 1988); ——, MO calculations (Allan 1986); ◆, experiment (Aumayr *et al* 1987); ◇, experiment (Dubois and Toburen 1985). Charge exchange cross section $\sigma_{3s}(2p)$: — —, AO calculations (Shingal *et al* 1986); ----, AO calculations (Fritsch 1988); – – –, MO calculations (Allan 1986); ▲, experiment (Aumayr *et al* 1987); +, experiment (Finck *et al* 1988).

$C=$CM than $C=$H, especially the cross sections $|3p\Pi^+\rangle \rightarrow |2p\Pi^+\rangle$ and $|3p\Pi^+\rangle \rightarrow |2p\Sigma\rangle$. Over *all* the range of energy studied, 0.35-5 keV, the two kinds of calculations ($C=$CM and $C=$H) give different charge exchange cross sections. The calculation with CTF again lies at the mean value between the two calculations without CTF. For this near-resonant transition $Na(3p) \rightarrow H(n=2)$ the molecular expansion without CTF is very dependent on the choice of the coordinate centre even at the lowest energy explored, 0.35 keV. Use of the CTF is therefore essential, and yields results in close agreement with recent experimental work (accompanying paper) as we shall see in section 3.2.3.

3.2. Molecular expansion with CTF

3.2.1. Dependence of the total cross sections on the translational factor. The parameter β introduced in the switching function of the CTF in (3) has been varied: $0<\beta<6$. As the β parameter is such that the CTF drops to zero at short distances it can be

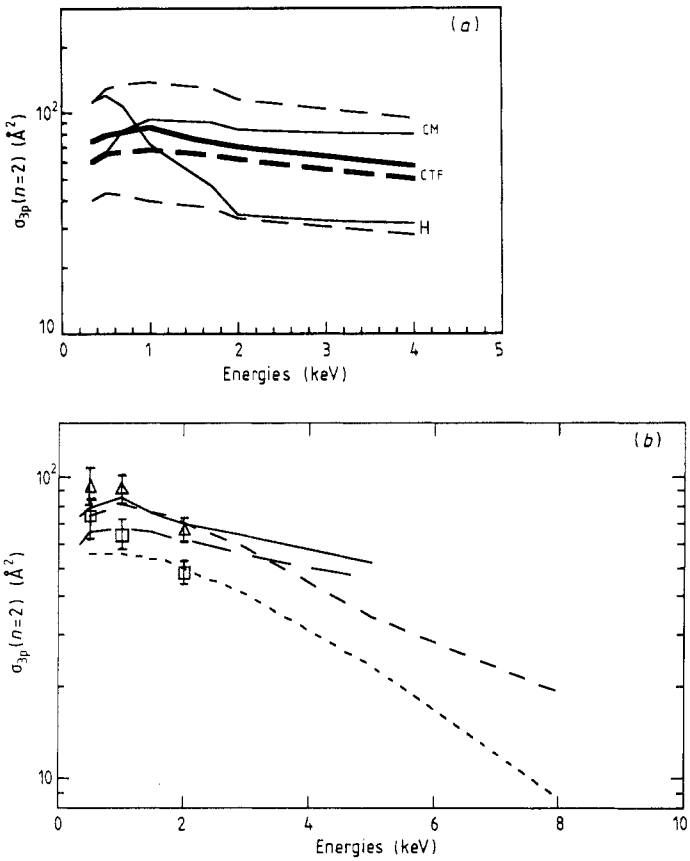

Figure 4. (*a*) Cross sections $\sigma_{3p\Sigma}(n=2)$: ——, without CTF and $C=H$; ——, with CTF; ——, without CTF and $C=CM$. Cross section $\sigma_{3p\Pi}(n=2)$: — — —, without CTF and $C=CM$; — — —, with CTF; — — —, without CTF and $C=H$. (*b*) $\sigma_{3p\Sigma}(n=2)$: ——, present results; – – –, AO (Fritsch 1988); △, experiment (Dowek *et al* 1990). $\sigma_{3p\Pi}(n=2)$: — — —, present results; ----, AO (Fritsch 1988); □, experiment (Dowek *et al* 1990).

expected that transitions occurring in the molecular region will be affected by the parameter of the switching function. The various cross sections vary by only a few per cent. The most sensitive one is $\sigma_{3s}(2s\Sigma)$ which varies by 10%. This transition is one which occurs at intermediate distances: $R<8$ au.

3.2.2. Comparison between the 9-state and the 19-state models. We compare $\sigma_i(n=2)$ cross sections calculated with two different collisional bases. The 9-state basis includes the channels Na(3sΣ, 3pΣ, 3pΠ^+, 3pΠ^-, 4sΣ), H(2sΣ, 2pΣ, 2pΠ^+, 2pΠ^-). The 19-state basis includes these nine states and Na(3dΣ, 4pΣ, 3dΠ^+, 3dΠ^-) and H(3sΣ, 3pΣ, 3pΠ^+, 3pΠ^-, 3dΠ^+, 3dΠ^-). $\sigma_\Sigma(n=2)$ and $\sigma_\Pi(n=2)$ are reported in table 1 for the 9-state model and table 2 for the 19-state model (and also compared with the atomic calculations of Fritsch (1988)). When $E<1$ keV the molecular 19-state results are similar to the 9-state results. When $E>1$ keV the charge exchange cross sections are 15% smaller in the 19-state model than in the 9-state one, this shows the limitations of the 9-state model and the important role of the $H(n=3)$ states at higher energies: the $H(n=3)$ capture or $Na(n=3)$ excitation is predicted to be important at $E>1$ keV. At $E>4$ keV

Table 1. State-to-state total cross section (Å^2) in the 9-state model: initial state $|Na, 3l\lambda\rangle$; final state, $|H, 2l'\lambda'\rangle$.

E_{lab} (keV)	0.35	0.5	1	1.5	2	3	4	5
v (au)	0.1183	0.1414	0.2000	0.2449	0.2828	0.3464	0.4000	0.4472
$3s\Sigma$-$2s\Sigma$	3.08	6.86	17.38	19.28	19.51	18.94	18.20	17.43
$3s\Sigma$-$2p\Sigma$	2.66	3.42	11.35	17.44	22.73	29.70	30.37	28.19
$3s\Sigma$-$2p\Pi^+$	6.7	7.42	8.29	6.71	7.09	11.74	16.38	19.32
$3p\Sigma$-$2s\Sigma$	22.45	17.06	21.89	28.92	30.06	29.19	28.90	28.77
$3p\Sigma$-$2p\Sigma$	25.84	31.70	24.93	13.51	7.93	6.82	8.31	9.21
$3p\Sigma$-$2p\Pi^+$	30.64	38.18	49.75	47.52	43.79	39.63	38.63	38.96
$3p\Pi^+$-$2s\Sigma$	21.64	25.89	30.49	29.65	28.48	25.62	22.48	19.70
$3p\Pi^+$-$2p\Sigma$	9.57	10.56	14.84	18.32	20.75	23.96	25.52	25.85
$3p\Pi^+$-$2p\Pi^+$	27.12	33.34	45.46	48.78	45.78	36.35	28.88	23.79
$3p\Pi^-$-$2p\Pi^-$	66.25	70.90	73.43	68.79	63.24	54.80	48.57	43.62
$\sigma_{3s\Sigma}(n=2)$	12.44	17.71	37.02	43.42	49.33	60.38	64.96	64.93
$\sigma_{3p\Sigma}(n=2)$	78.93	86.94	96.58	89.95	81.78	75.64	75.85	76.94
$\sigma_{3p\Pi^+}(n=2)$	58.33	69.79	90.80	96.76	95.01	85.93	76.89	69.35
$\sigma_{3p\Pi}(n=2)$	62.29	70.34	85.00	79.37	79.12	70.36	62.73	56.48

Table 2. State-to-state total cross section (Å^2) in the 19-state model: initial state, $|Na, 3, l\lambda\rangle$; final state, $|H, 2l'\lambda'\rangle$; a, atomic orbital calculations of Fritsch (1988).

v (au)	0.1183	0.1414	0.2000	0.2449	0.2828	0.3464	0.4000	0.4472
$3s\Sigma$-$2s\Sigma$	3.10	6.23	15.57	17.26	18.02	17.94	16.88	15.57
$3s\Sigma$-$2p\Sigma$	2.48	3.26	10.94	16.17	20.42	25.31	25.57	24.19
$3s\Sigma$-$2p\Pi^+$	6.98	7.47	8.54	5.77	5.53	8.89	11.55	12.94
$3p\Sigma$-$2s\Sigma$	23.12	16.46	21.84	26.57	28.20	26.77	22.83	18.77
$3p\Sigma$-$2p\Sigma$	25.16	30.50	22.29	9.04	5.38	6.44	8.03	9.21
$3p\Sigma$-$2p\Pi^+$	25.98	32.01	41.88	40.60	36.63	30.45	26.67	23.90
$3p\Pi^+$-$2s\Sigma$	21.49	26.07	21.45	17.89	15.25	12.34	10.32	9.16
$3p\Pi^+$-$2p\Sigma$	11.07	8.91	13.40	19.43	22.33	21.79	19.08	16.80
$3p\Pi^+$-$2p\Pi^+$	22.77	26.83	29.00	27.81	26.47	24.69	22.77	20.83
$3p\Pi^-$-$2p\Pi^-$	65.16	69.51	72.38	66.20	59.48	52.03	48.02	45.03
$\sigma_{3s\Sigma}(n=2)$	12.56	16.96	35.06	39.21	43.98	52.13	53.99	52.69
$\sigma_{3s\Sigma}(n=2)^a$		10.66	28.03	37.90†		56.38		48.76
$\sigma_{3p\Sigma}(n=2)$	74.26	78.98	86.01	76.21	70.21	63.66	57.53	51.88
$\sigma_{3p\Sigma}(n=2)^a$		74.57	81.18	74.8†		58.16		34.30
$\sigma_{3p\Pi^+}(n=2)$	55.33	61.81	63.84	65.13	64.06	58.82	52.18	46.80
$\sigma_{3p\Pi}(n=2)$	60.2	65.6	68.1	65.6	61.8	55.4	50.1	45.9
$\sigma_{3p\Pi}(n=2)^a$		52.40	55.70	54.07†		42.88		24.95

† Values corresponding to $E_{lab} = 1.7$ keV.

both the $\sigma_\Sigma(n=2)$ and $\sigma_\Pi(n=2)$ cross sections are about a factor of two larger than the 49-state result of Fritsch (1988).

3.2.3. Electron capture from Na(3s). The metastable fraction $f_{2s} = \{H(2s)\}/\{H(n=2)\}$ has been calculated in the 9- and 19-state models after analytically integrating the long-range Stark and rotational coupling (see section 2.1). A comparison of the present result with the preceding calculation of I where the coupled equations were numerically integrated up to $z_{max} = 95$ au is shown in table 3. The fraction is not sensitive to the

Table 3. Metastable fraction $f_{2s} = \{H(2s)\}/\{H(n=2)\}$ for reaction (R1). The present results: a, for the 9-state model; b, for the 19-state model; c, results of I (19 states).

v (au)	0.1183	0.1414	0.2000	0.2449	0.2828	0.3464	0.4000	0.4472
$f_{2s}{}^{a}$	0.25	0.39	0.47	0.44	0.39	0.31	0.28	0.27
$f_{2s}{}^{b}$	0.245	0.37	0.44	0.44	0.40	0.34	0.31	0.29
$f_{2s}{}^{c}$		0.37	0.42	0.43	0.44	0.42	0.40	0.38

number of states included in the model but it is sensitive to the treatment of the asymptotic region. The present result with 19 states including the exact treatment of the long-range coupling must be considered as the most accurate.

Figure 3(b) shows the total cross section for the processes:

$$H^+ + Na(3s) \rightarrow H(2p) + Na^+ \qquad (R3)$$

$$H^+ + Na(3s) \rightarrow H(\Sigma n) + Na^+. \qquad (R4)$$

For total electron capture the present results are consistent with the AO results of Shingal *et al* and Fritsch (1984) up to $E = 5$ keV. At $E < 2$ keV the AO results are a few per cent lower than the present MO results, but no experimental values are available in this energy range with which to compare. At $E > 6$ keV the two sets of experimental results (Aumayr *et al* 1987, Dubois and Toburen 1985) are very similar and in very good agreement with both AO results.

For capture into the H(2p) state the two recent Ly_α measurements agree very well. The two sets of AO and MO results are in close agreement with the experiments. However at $E < 0.5$ keV the present $\sigma_{3s}(2p)$ is found larger by a factor of two than the AO calculations. The experimental points confirm the AO result.

As in this energy range the CTF has been shown not to play any role (see section 3.1) the discrepancy between the two models can only be attributed to the number of states: it means that the couplings to the higher states of the system are important despite the low energy.

As all the H($n = 3$) states are not included in the present model ($3d\Sigma_H$ for instance), the capture cross sections to H($n = 3$) can only be considered as a qualitative result. The $\sigma_{3s}(n = 3)$ charge exchange cross section to H($n = 3$) is compared with the atomic calculations (table 4) of Fritsch (1984): the agreement is surprisingly good between theories, and the theoretical results are within the experimental error bars (Royer *et al* 1988). The cross section $\sigma_{3s}(n = 3)$ is small: it varies between 0.3 Å^2 and 8 Å^2.

Table 4. State-to-state total cross section (Å^2) in the 19-state model; initial state, |Na, 3 0 0⟩; final state |H, 3 l λ⟩; a, atomic orbital results of Fritsch (1988).

v (au)	0.1183	0.1414	0.2000	0.2449	0.2828	0.3464	0.4000	0.4472
$3s\Sigma$-$3p\Sigma$	0.097	0.198	0.854	1.32	1.52	2.13	2.18	2.36
$3s\Sigma$-$3d\Sigma$	0.03	0.035	0.43	0.46	0.70	0.87	0.68	0.83
$3s\Sigma$-$3p\Pi^+$	0.11	0.16	0.32	0.65	1.09	2.21	2.93	3.12
$3s\Sigma$-$3d\Pi^+$	0.04	0.105	0.26	0.40	0.51	0.68	1.05	1.43
$\sigma_{3s\Sigma}(n = 3)$	0.27	0.50	1.87	2.83	3.83	5.89	6.85	7.74
$\sigma_{3s\Sigma}(n = 3)^a$		0.8	1.80	4.07†		8.08		11.14

† Value corresponding to $E_{lab} = 1.7$ keV.

3.2.4. Electron capture from Na(3p) excited by a linearly polarized light.* The linearly polarized exciting light prepares the atomic orbitals in a linear combination of $m_L = 0$ (Σ) and ± 1 (Π) states, depending on its two polarization directions (parallel or perpendicular to the proton beam) and not in a pure state because of the hyperfine structure (Dowek *et al* 1990). The experimental technique used gives the ratio of $\sigma_{3p}(n=2)$ to the $\sigma_{3s}(n=2)$ cross section. Relations between the measured cross sections and $\sigma_\Sigma(n=2)$ and $\sigma_\Pi(n=2)$ are given by formulae (2*a*) and (2*b*) in the following paper (Richter *et al* 1990). The $\sigma_{3p\Sigma}(n=2)$ and $\sigma_{3p\Pi}(n=2)$ experimental cross sections are therefore drawn in figure 4(*b*), after being calibrated to the reliable $\sigma_{3s}(n=2)$ cross section, from the large AO basis expansion (Fritsch 1984, Shingal *et al* 1986). In this figure is also drawn the present 19 molecular state result and the AO basis result of Fritsch (1988), the only theoretical results available for $\sigma_{3p\Sigma}(n=2)$ and $\sigma_{3p\Pi}(n=2)$. The $\sigma_{3p\Sigma}(n=2)$ cross section is the larger in both calculations, compared with $\sigma_{3p\Pi}(n=2)$. The two calculations and the experimental points are in good agreement. From values tabulated (table 2), the calculated $\sigma_{3p\Pi}(n=2)$ is found to be 20% smaller than $\sigma_{3p\Sigma}(n=2)$, this is a strong alignment effect in the keV energy range.

4. Charge exchange probabilities and differential cross sections

4.1. Charge exchange probabilities from Na(3s)

For the exchange channels $H(2s\Sigma)$, $H(2p\Sigma)$, $H(2p\Pi^+)$ the capture probabilities are drawn as a function of the impact parameter at the energy $E_{lab} = 0.5$ keV (figure 5(*a*)) and 2 keV (figure 6(*a*)); the main features are the two peaks at $R = 7.5$ au and 12 au for the $H(2s\Sigma)$ and $H(2p\Sigma)$ probabilities. The energy difference $E_{3s\Sigma} - E_{2s\Sigma} \simeq 0.05$ au has the same value as the corresponding $\frac{1}{2}H_{ij}$ at $R \simeq 7$ au and $R \simeq 12$ au. The population of the $H(2s\Sigma)$ and $H(2p\Sigma)$ channels can thus be explained as a direct transition induced by the dynamical H_1 radial coupling. The population of $H(2p\Pi^+)$ becomes important at quite short distances, $4 < R < 6$ au, where indeed the matrix element is large, $\langle 3s\Sigma | H_2 | 2p\Pi^+ \rangle \simeq 0.5$ au. At $E = 2$ keV its population is enhanced as the effect of the rotational coupling increases with collision velocity. Thus the $H(2p\Pi^+)$ state is populated via a direct rotational coupling.

It must be stressed that the charge exchange reaction (R1) takes place in an intermediate region $5 < R < 12$ au as the transition is non-resonant, which explains the weak total cross sections (< 50 Å^2). We shall see how it is different for the capture from $Na^*(3p)$ states.

4.2. Charge exchange probabilities from Na(3p)*

From the $Na(3p\Sigma)$ state, the charge exchange probability for populating $H(2p\Pi^+)$ (shown in figures 5(*b*) and 6(*b*)) is interpreted as a direct rotational coupling at $10 < R < 15$ au, since $|\langle 3p\Sigma | H_2 | 2p\Pi^+ \rangle| \simeq 0.3$ au in this region (figure 2(*b*)). The large population of $H(2s\Sigma)$, (0.3 at 0.5 keV and 0.2 at 2 keV) is explained by a direct transition through the radial coupling $|\langle 3p\Sigma | H_1 | 2s\Sigma \rangle| \simeq 0.03$ au (figure 2(*a*)) equal to $E_{3p\Sigma} - E_{2s\Sigma}$ at $R \simeq 12$ au. The $H(2p\Sigma)$ population is smaller than the $H(2s\Sigma)$ population in the energy range $E > 0.5$ keV.

From the $Na(3p\Pi^-)$ initial state, only the final state $H(2p\Pi^-)$ of $H(n=2)$ can be populated (figures 5(*c*) and 6(*c*)) via the radial coupling $\langle 3p\Pi^- | H_1 | 2p\Pi^- \rangle$. The charge

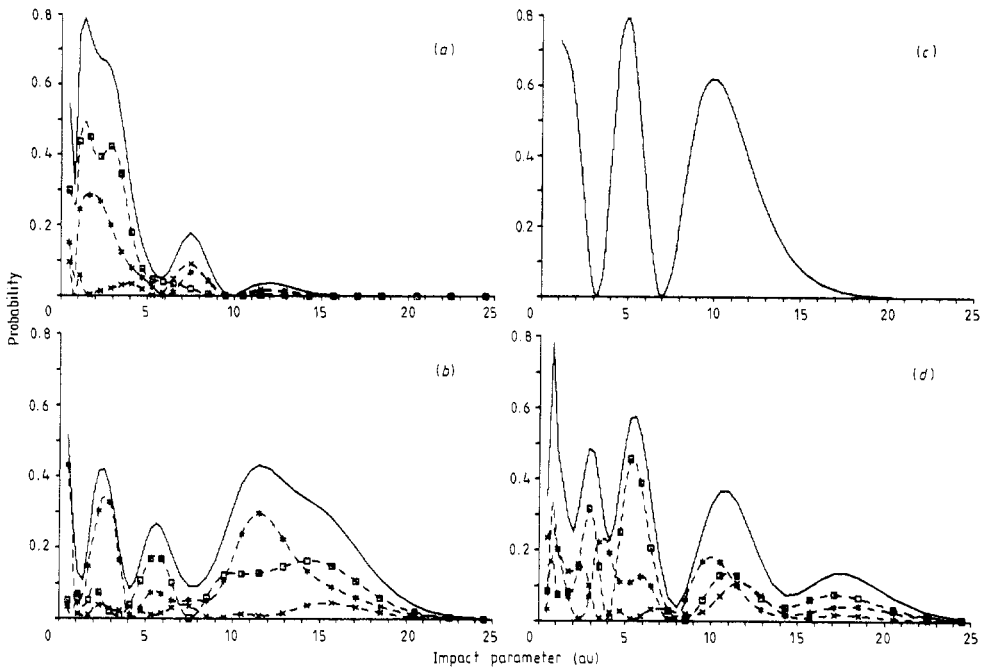

Figure 5. Charge exchange probabilities as a function of the impact parameter in the 9-state model at $v = 0.14$ au. (a) The initial state $|3s\Sigma_{Na}\rangle$. The final state: $--*--$, $|2s\Sigma_H\rangle$; $--\times--$, $|2p\Sigma_H\rangle$; $--\square--$, $|2p\Pi_H^+\rangle$; ——, sum over the states $H(n=2)$. (b) The initial state $|3p\Sigma_{Na}\rangle$ and the same notations as in (a). (c) The initial state $|3p\Pi_{Na}^-\rangle$ and the final state $|2p\Pi_H^-\rangle$. (d) The initial state $|3p\Pi_{Na}^+\rangle$ and the same notations as in (a).

exchange radial coupling of Demkov type between the two states gives rise to a structure peak at $R \simeq 11$ au typical of a pseudo-crossing occurring at $R \simeq 12$ au.

From the $Na(3p\Pi^+)$ state the largest population is the $H(2p\Pi^+)$ (figures 5(d) and 6(d)), it has a maximum at $R \simeq 11$ au and at $R = 17.5$ au. By analogy with the population of $H(2p\Pi^-)$ from the initial state $Na(3p\Pi^-)$ (figures 5(c) and 6(c)) it can be said that the peak at $R = 11$ au is due to the same mechanism as a direct transition through the dynamical $\langle 3p\Pi^+|H_1|2p\Pi^+\rangle$ coupling. However a more complex structure of the $H(2p\Pi^+)$ probability occurs; the peak at $R \simeq 17.5$ au can be a two-step transition through a rotational coupling $Na(3p\Pi^+) \rightarrow H(2p\Sigma)$ (as the $\langle 3p\Pi^+|H_2|2p\Sigma\rangle \simeq 0.5$ au at $13 < R < 20$ au, figure 2(b)) followed by the long-range rotational coupling $H(2p\Sigma) \rightarrow H(2p\Pi^+)$ transition. The probability $H(2s\Sigma)$ has a maximum at $R = 10$ au due to $\langle 3p\Pi^+|H_2|2s\Sigma\rangle$ if we refer to the shape of the corresponding rotational coupling (figure 2(b)).

The comparison of the probabilities between $v = 0.14$ au and $v = 0.283$ au shows that at higher collision velocity the probabilities are shifted to larger impact parameters, especially when the initial state is $|3s\Sigma_{Na}\rangle$. The three states $|2s\Sigma_H\rangle$, $|2p\Sigma_H\rangle$ and $|2p\Pi_H^+\rangle$ are equally populated when the initial state is $|3s\Sigma_{Na}\rangle$ or $|3p\Sigma_{Na}\rangle$, but at $E = 2$ keV the $|2p\Sigma_H\rangle$ state is weakly populated when the initial state is $|3p\Pi_{Na}^+\rangle$.

From figures 5 and 6 it is clear that charge exchange in this system from excited states takes place at quite large distances, $10 < R < 20$ au, as the reaction is near resonant, which explains the much bigger value of the charge exchange total cross section when the initial state is Na(3p) ($\simeq 80$ Å^2, see tables 1 and 2).

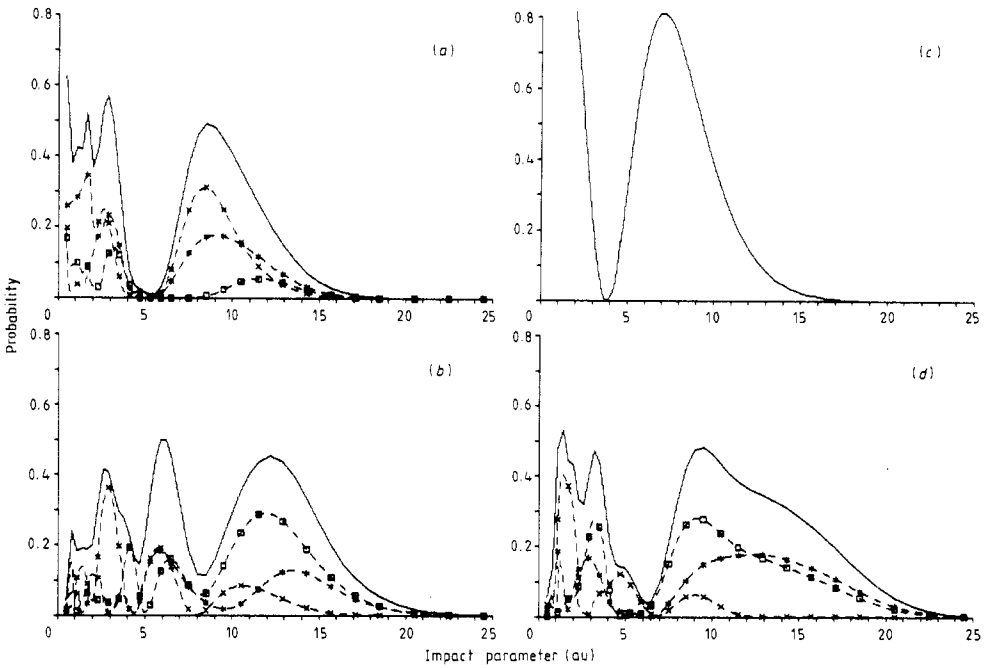

Figure 6. Charge exchange probabilities as a function of the impact parameter at $v = 0.283$ au, with the same notations for (a)-(d) as (a)-(d) in figure 5.

4.3. Differential cross sections

From the transition amplitudes the differential cross sections are calculated using the method of Piacentini and Salin (1977) at $E = 0.5$ keV and $E = 2$ keV for various initial states. At $E = 0.5$ keV (figure 7) the charge exchange differential cross sections are spread out to a scattering angle $\theta = 0.4°$, when at $E = 2$ keV (figure 8) they are spread out to an angle four times smaller (0.1°).

All the differential cross sections oscillate, due to rainbow effects in the long-range attractive part of the potential curves. The largest charge exchange cross sections are obtained from the initial state $|3p\Sigma_{Na}\rangle$ to the final states $|2p\Sigma_H\rangle$ and $|2p\Pi_H^+\rangle$ at $E = 0.5$ keV. Its average width is about 0.2°, it could be measured with less difficulty than the DCS at 2 keV, which is narrower due to kinematic effects. The difference in shape of the DCS in figures 7(b) and (c) is a differential alignment effect, its measurement would be of great interest as a test of our model. The differential orientation effect is also predicted (Allan *et al* 1990) in which it is interpreted as a velocity matching effect.

5. Conclusion

We have presented a detailed investigation of the electron capture to $H(n = 2)$ and $H(n = 3)$ through the 14 positive and 5 negative symmetry molecular states of the H^+-Na collisional system. The work has been stimulated by recent experiments where Na is prepared excited by a polarized laser light.

We have reviewed the current status of theoretical work on the NaH^+ system and highlighted the following points which are essential for a quantitative comparison. An

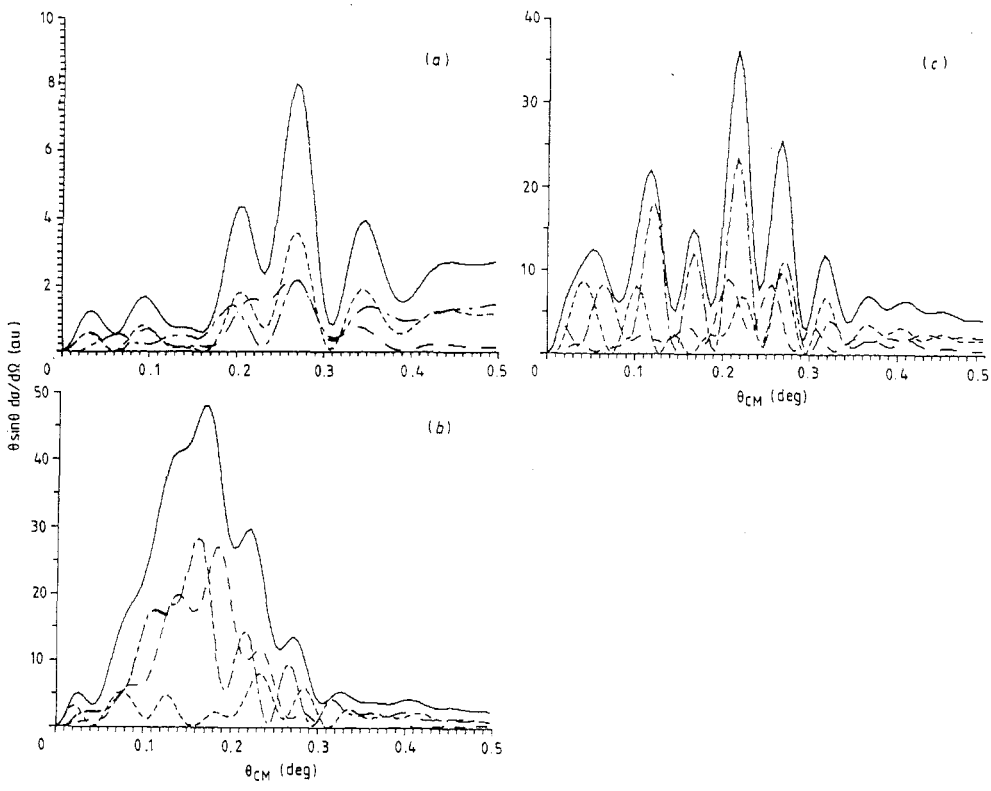

Figure 7. Differential charge exchange cross sections at $v = 0.14$ au. Initial state: (*a*) $|3s\Sigma\rangle$; (*b*) $|3p\Sigma\rangle$; (*c*) $|3p\Pi^+\rangle$. Final state: – – – –, $|2s\Sigma\rangle$; — — —, $|2p\Sigma\rangle$; — – —, $|2p\Pi^+\rangle$; ——, sum over the states H ($n = 2$).

electron translation factor must be incorporated into the MO treatment and a correct projection onto the asymptotic states must be used. Bearing this in mind, recent MO and AO calculations are now in good agreement, and of similar predictive power, however a sufficiently large number of states must be well understood within the MO model in terms of radial and rotational coupling and interference effects.

We have shown that the cross sections for state-to-state transitions are sufficiently large for experimental observation. Results of such an experiment are compared with our predictions in the accompanying paper.

Acknowledgments

The calculations were carried out on the Convex C220 and 64-node Intel iPSC/2 computers at Daresbury Laboratory (UK), on the IBM 3090 computers of the CIRCE in Orsay (France) and on the IBM 3090 of CIEMAT in Ciudad Universitaria of the Universidad Politecnica in Madrid (Spain).

One author (CC) is grateful to the Royal Society and the CNRS for financial support enabling her to visit Daresbury Laboratory from September 1987 to September 1988 and in 1989. PW and PS also thank the DG Investigacion Scientifica y Tecnica of Spain (PS 87-0097) for financial support. This work is supported under an EEC CODEST programme.

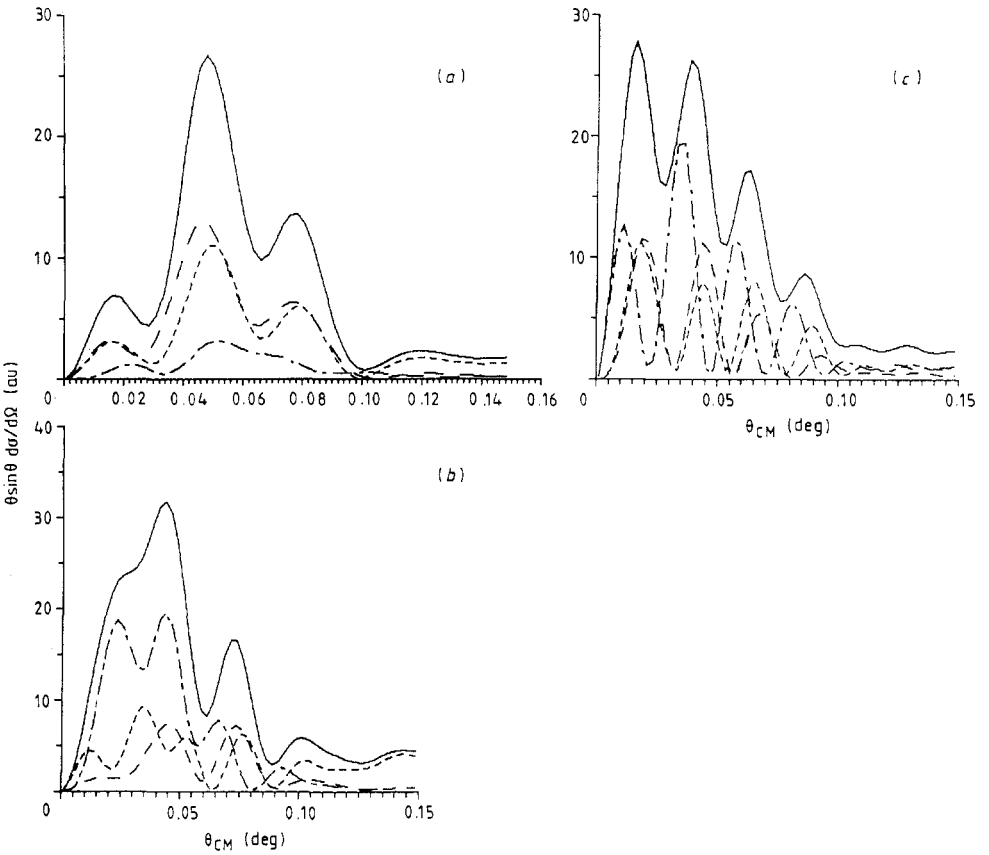

Figure 8. Differential cross sections at $v = 0.283$ au with the same notations as in figure 7.

References

Allan R J 1986 *J. Phys. B: At. Mol. Phys.* **19** 321-34

Allan R J, Courbin C, Salas P and Wahnon P 1990 *J. Phys. B: At. Mol. Opt. Phys.* **23** L461-6

Allan R J and Hanssen J 1985 *J. Phys. B: At. Mol. Phys.* **18** 1981-97

Allan R J, Shingal R and Flower D R 1986 *J. Phys. B: At. Mol. Phys.* **19** L251-6

Anderson C J, Howald A M and Anderson L W 1979 *Nucl. Instrum. Methods* **165** 583-7

Aumayr F and Winter H 1987 *J. Phys. B: At. Mol. Phys.* **20** L803-7

Aumayr F, Latikis G and Winter H 1987 *J. Phys. B: At. Mol. Phys.* **20** 2025-30

Dowek D, Houver J C, Pommier J, Richter C, Andersen N and Palsdottir B 1990 *Phys. Rev. Lett.* **64** 1713-6

Dubois R D and Toburen L H 1985 *Phys. Rev.* A **31** 3603-11

Ebel and Salzborn E 1983 *Proc. 13th Int. Conf. on Physics of Electronic and Atomic Collisions (Berlin)* ed J Eichler *et al* (Amsterdam: North-Holland) Abstracts p 491

Errea L F, Mendez L and Riera A 1982 *J. Phys. B: At. Mol. Phys.* **15** 101-10

Finck K, Wang Y, Roller-Lutz Z and Lutz H O 1988 *Phys. Rev.* A **38** 6115-9

Fritsch W 1984 *Phys. Rev.* A **30** 1135-8

—— 1988 private communication

Gruebler W, Schmelzbach P A, König V and Marnier P 1970 *Helv. Phys. Acta* **3** 254-71

Kimura M, Olson R E and Pascale J 1982a *Phys. Rev.* A **26** 1138-41

—— 1982b *Phys. Rev.* A **26** 3113-24

Kubach C and Sidis V 1981 *Phys. Rev.* A **23** 110-8

Kushawaha V S 1983 *Z. Phys.* A **313** 155-60

Kushawaha V S, Burkhardt C E and Leventhal J S 1980 *Phys. Rev. Lett.* **45** 1686-8
McCullough R W 1978 unpublished results
Nagata T 1983 *Proc. 13th Int. Conf. on Physics of Electronic and Atomic Collisions (Berlin)* ed J Eichler *et al* (Amsterdam: North-Holland) Abstracts p 490
Piacentini R D and Salin A 1977 *Comput. Phys. Commun.* **13** 57-62
Richter C, Dowek D, Houver J P and Andersen N 1990 *J. Phys. B: At. Mol. Opt. Phys.* **23** 3925-32
Royer T, Dowek D, Houver J C, Pommier J and Andersen N 1988 *Z. Phys. D* **10** 45-57
Schneiderman S B and Russek A 1969 *Phys. Rev.* **181** 311-21
Shingal R, Bransden B H, Ermolaev A M, Flower D R, Newby C W and Noble C J 1986 *J. Phys. B: At. Mol. Phys.* **19** 309
Sidis V and Kubach C 1978 *J. Phys. B: At. Mol. Phys.* **11** 2687-703
Taulbjerg K and Briggs J S 1975 *J. Phys. B: At. Mol. Phys.* **8** 1895-908
Wahnon P, Gala S, Duro M C, Courbin-Gaussorgues C and Sidis V 1986 *J. Phys. B: At. Mol. Phys.* **19** 611-28